High-Speed Real-Time Dynamic Economic Load Dispatch

Naoto Yorino, *Member, IEEE*, Habibuddin M. Hafiz, *Student Member, IEEE*, Yutaka Sasaki, *Member, IEEE*, and Yoshifumi Zoka, *Member, IEEE*

***Abstract*—A large amount of renewable energy penetration may cause a serious problem in load dispatch in the future power system, where the amount of controllable generators will decrease while disturbances increase. Therefore, a new economic load dispatch (ELD) method is required in order to make the best use of the ramp-rate capability of existing generators to cope with the disturbances caused by loads as well as by renewable energy generations. This paper proposes a new dynamic ELD method to meet the general requirements for real-time use in a future power system, where load following capability is critically limited. The method is also satisfactory from an economical point of view, and is suitable for high-speed online application due to fast and steady computation time. The proposed method has been successfully tested on several systems supplying a typical morning to noon demand profile.**

***Index Terms*—Dynamic economic dispatch, feasible operation region, reserve.**

I. Introduction

RECENTLY various problems have arisen due to penetration of renewable energy generations in electric power systems. In Japan, 53 GW of photovoltaic (PV) generations are expected to be installed until 2030. This numeric corresponds to 20% of peak demand in light load season, where the amount of controllable generators will be so limited that load following capability will be a serious problem. A key issue for secure operation in such a power system is how to deal with unpredictable output of PV generation by using available limited amount of controls. It is expected that the role of thermal power plants will increase for this purpose, and thus, robust and reliable load dispatching method will be required. In other words, new type of method for dynamic economic load dispatch (DELD) is necessary to deal with sudden change in PV generation in real-time operations.

Various approaches have been proposed so far concerned with the DELD problem. DELD looks ahead over the future time horizon using future load forecast to determine the economic allocation of generation to the load [1]. It also takes into account the dynamic constraints of generators such as dynamic ramp-rate in the optimization process [2]. The heuristic technique developed in [3] is useful because of its simplicity even though not necessarily optimal. References [4] and [5] use the simulated annealing in the DELD problem. Hybrid algorithm was proposed in [6] consisting the Hopfield neural network and quadratic programming (QP). A price-based ramp-rate model has been proposed in [7] for application to power system scheduling models that are based on dual-formulation. For large scale DELD problem, [8] proposed the application of variable scaling hybrid differential algorithm. Reference [9] proposes a re-dispatch algorithm using QP combined with linear programming (LP) and the Danzig Wolfe's decomposition technique. Reference [10] uses multi-stage approach by adding ramp-rate constraint to the extended security constrained DELD. The interior point method was used to tackle the problem as a single optimization problem in [11]. Since in many cases no feasible solutions can be guaranteed, a heuristic method is proposed in [12] to improve the feasibility even when the load profile is non-monotonic.

Although those conventional approaches have been effective so far for conventional power systems, a new approach is required in future power systems, where demand patterns are more uncertain and amount of conventional controllable generators are critically decreased. Conventional approaches assumed that the demand is feasible for dispatch and also that generation schedule (GS) does not change much. In cases with high penetration of renewable energy, high fluctuation might cause the load to be infeasible for dispatch, and forecast error will require change in GS. Therefore, in a real-time application, GS should be updated frequently to cope with change in forecasted load and renewable generation as well as ensuring dispatch feasibility. Hence, there is a need for a method that can address the issue of infeasibility and GS change reliably in a very fast manner. Thus, the computation speed is the critical issue to deal with the disturbance caused by the renewable energy resources.

This paper proposes a new real-time DELD method. Based on investigation of future circumstance, it is preferable that all computational process in the control center is automatic and that the individual local generators under the central control can obtain their direct control signals and their GS for a specific time interval. Therefore, in the proposed method, GS is always recalculated and updated in every real-time control cycle to deal with sudden change in load prediction as well as weather forecast. The time duration for the real-time GS is referred to as time

Manuscript received September 14, 2010; revised March 21, 2011 and July 14, 2011; accepted September 13, 2011. Date of publication October 19, 2011; date of current version April 18, 2012. Paper no. TPWRS-00742-2010.

N. Yorino, Y. Sasaki, and Y. Zoka are with the Electric Power and Energy System Laboratory, Graduate School of Engineering, Hiroshima University, 739-8524 Hiroshima, Japan (e-mail: yorino@hiroshima-u.ac.jp; yusasaki@hiroshima-u.ac.jp; zo@hiroshima-u.ac.jp).

H. M. Hafiz is with the Faculty of Electrical Engineering, Universiti Teknologi Malaysia, 81310 UTM Skudai, Malaysia, on leave to study at the Electric Power and Energy System Laboratory, Graduate School of Engineering, Hiroshima University, 739-8527 Hiroshima, Japan (e-mail: mhafiz@fke.utm.my).

Digital Object Identifier 10.1109/TPWRS.2011.2169285

horizon in this paper. The proposed method has the following characteristics:

1) cost minimization and real-time GS computation over the entire specified time horizon;
2) a new formulation using the ramp rate variables make possible the use of the conventional equal incremental fuel cost method (equal λ method), resulting in much faster processing speed than the conventional QP with little compromising the objective;
3) in the update process of GS, change in generation is minimized (high dependability for the operators);
4) supply-demand balance in the entire time horizon is kept to the maximum (high feasibility of dispatch);
5) the method is advantageous for a critical situation where the forecasted load cannot be matched by the existing generator's capability. In this case, the method will detect the minimum amount of supply-demand mismatch (SDM) in advance and reliably treat it in the considered time horizon.

II. Outline of the Proposed Method

A. Objective Function and Constraints

The objective function for DELD problem is given by quadratic functions with N controllable generators in a time horizon of T intervals ahead of current time:

$$\left.\begin{aligned} f &= \textstyle\sum_{t=1}^{T} f_t \\ f_t &= \textstyle\sum_{k=1}^{N} \left(\frac{a_k}{2} P_{kt}^2 + b_k P_{kt} + c_k\right) \\ &= \tfrac{1}{2} P_t^T A P_t + b^T P_t + \textstyle\sum_{k=1}^{N} c_k \end{aligned}\right\}. \tag{1}$$

The following constraints are assumed:

1) Supply-demand balance constraint

$$\sum_{k=1}^{N} P_{kt} = \hat{P}_t \tag{2}$$

2) Generator capacity constraint

$$\underline{P}_k \le P_{kt} \le \bar{P}_k \tag{3}$$

3) Ramp-rate constraint

$$-\delta_k \le P_{kt} - P_{k(t+1)} \le \delta_k \tag{4}$$

where $P_t = [P_{1t} \cdots P_{Nt}]^T$; $A = diag\,[a_1 \cdots a_N]$; $b = [b_1 \cdots b_N]$; f_t is the generation cost at time point t; P_{kt} is the output of generator k at time point t (MW); a_k, b_k, and c_k are the quadratic cost coefficient of generator k; $\hat{P}_t$ is the forecasted demand at time point t (MW); $\bar{P}_k$ and $\underline{P}_k$ are the upper and lower generation limit of generator k; and δ_k is the ramp-rate limit of generator k (MW/unit time). Note that we use the index $t = T$ at the present time point and decreasing to $t = 1$ at the end point of the time horizon. We use reverse notation for the time point since the main algorithm (Section II-C) is performed backward from the end point of the time horizon towards present time point.

B. Brief Explanation of the Proposed Method

The proposed method involves four stages. The first stage is the GS shift. In this stage, GS calculated in the previous control cycle is shifted to the current time horizon. Then, in the next stage, feasible operation region and supply demand mismatch are determined using the latest load forecast in the current time horizon. In the third stage, we determine the dispatch value at the end of the time horizon. In the final stage, which is the main algorithm, we determine the correction of base GS of the entire time horizon. These four stages are described in the following sub-sections. The flowchart of the detailed algorithm is given in Fig. 1, which will be explained throughout the paper.

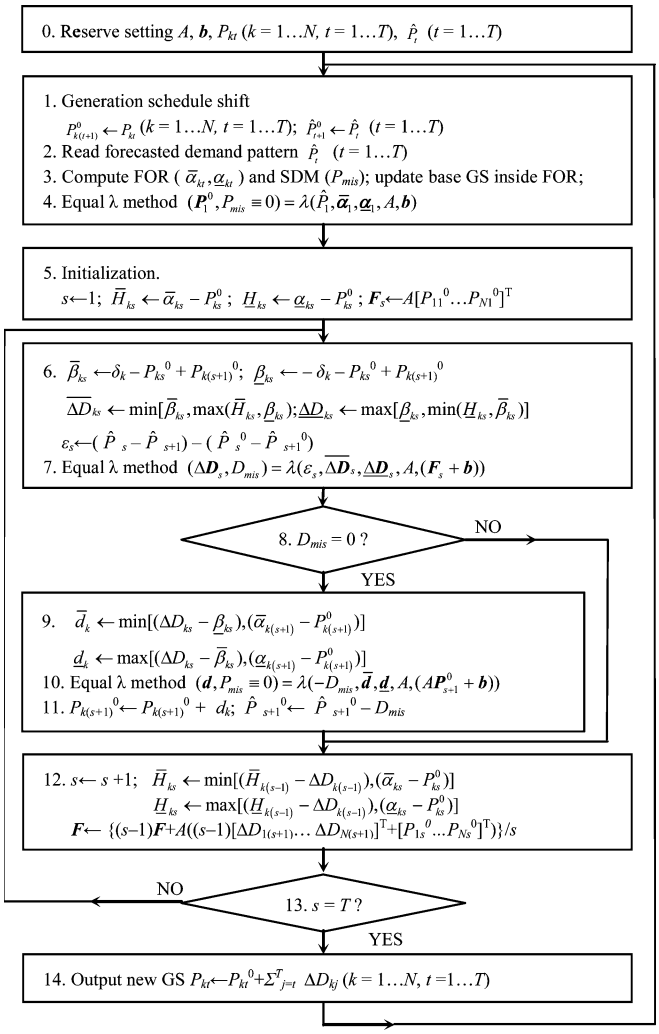

Fig. 1. Algorithm of the proposed method.

1) GS Shift: Fig. 2(a) shows GS (A, A'-A") determined by the computation in previous control cycle within a time horizon of over T intervals. It is assumed in this paper that one interval corresponds to 5 min and $T = 12$, implying one hour GS in every 5 min. Here, the value "A" is the present active power output of generator k, and A'-A" are GS in the succeeding instants. As explained in issue 5) in the Introduction, the method calculates the SDM, denoted as P_{mis}. In the fully automated process of the proposed method, P_{mis} is compensated by the reserve prepared in the system. This may includes non-spinning reserve, power import, or load shedding. However, this paper will not intentionally discuss how the compensation will be performed, but the behavior of P_{mis} with respect to time will be analyzed to show the reliability of the proposed method.

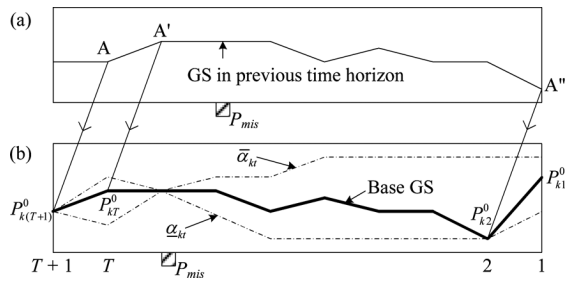

Fig. 2. GS shift and feasible operation region over a time horizon.

In this stage, GS is shifted by 1 interval such that A and A'-A" is shifted 1 interval to the left as shown in Fig. 2(b). Each dispatch value is designated as $P^0_{k(T+1)}, P^0_{kT}, \ldots$, and P^0_{k2}, which will be called the base GS [bold line in Fig. 2(b)]. Note that $P^0_{k(T+1)}$ at A is the active power output of the kth generator at the current time point, while A'-A" are written as $P^0_{kt}(t = T \ldots 1)$. The shift in GS is described as step 1 in Fig. 1.

2) Calculation of FOR and Supply-Demand Mismatch: Feasible operation region (FOR) is defined as the region of generator output P_{kt} reachable from a specified operating point, satisfying all the constraints (2)–(4) with load forecasts for $t = 1 \ldots T$. An algorithm to obtain the FOR is proposed in [13], where the present operating point, $P^0_{k(T+1)}$, a fixed point at $t = T + 1$, is used as starting point to obtain reachable points successively in forward direction to $t = 1$. Using the algorithm, the upper feasible operation limit $\bar{\alpha}_{kt}$ and lower feasible operation limit $\underline{\alpha}_{kt}$ are calculated for each committed generator $k = 1 \ldots N$ [dash-dotted line in Fig. 2(b)] using the latest forecasted demand $\hat{P}_t(t = 1 \ldots T)$. The FOR is the area inside the dash-dotted line in Fig. 2(b). In this way, once the upper and lower limits are obtained, any output value P_{kt} inside the limits

$$\underline{\alpha}_{kt} \le P_{kt} \le \bar{\alpha}_{kt} \tag{5}$$

is guaranteed as reachable under the latest load forecast. In this algorithm, when $\bar{\alpha}_{kt} < \underline{\alpha}_{kt}$ is detected, FOR is nonexistent, and the SDM can be computed. The calculation of FOR and SDM corresponds to step 2 and 3 in Fig. 1.

3) Calculation of Base Dispatch Value at Time $t = 1$: The base dispatch value at time point $t = 1$, P^0_{k1}, is determined by using equal incremental fuel cost method (equal λ method) subject to the forecasted demand $\hat{P}_1$. P^0_{k1} must be within upper and lower limits $\bar{\alpha}_{k1}$ and $\underline{\alpha}_{k1}$ of the FOR:

$$\underline{\alpha}_{k1} \le P^0_{k1} \le \bar{\alpha}_{k1}. \tag{6}$$

The equal λ method is generally accepted as a fast way to determine the dispatch value that matches the power demand in a way that the cost is minimized and the dispatch value lies within specified limits. The explanation for the equal λ method used in this paper is given in [14]. If the demand cannot be matched, the algorithm computes the amount of mismatch P_{mis} and the dispatch value $P^0_1 = \left[P^0_{11} \cdots P^0_{N1}\right]$ within the specified limits. The equal λ method subroutine will be used with forecasted demand $\hat{P}_1$, vectors of limits $\bar{\alpha}_1$, $\underline{\alpha}_1$ defined in (6), and fuel cost coefficients defined in (1) as inputs. The use of this subroutine is expressed as in the following form throughout this paper:

$$\left(P^0_1, P_{mis} \equiv 0\right) = \lambda\left(\hat{P}_1, \bar{\alpha}_1, \underline{\alpha}_1, A, b\right). \tag{7}$$

Note that, since the calculation is done inside the FOR, P_{mis} is always guaranteed as zero. In this sense, we use the notation of $P_{mis} \equiv 0$. The calculation of P^0_{k1} is described as step 4 in Fig. 1.

4) Correction of Base GS: The base GS, $P^0_{k(T+1)}, \ldots, P^0_{k2}$, P^0_{k1} were defined in the previous section, where P^0_{k1} is given by (7) and the others are based on the load forecast in the previous time horizon. Note that the transition from P^0_{k2} to P^0_{k1} does not meet the ramp-rate constraint. Then the base GS will be updated by adding $\Delta P_{kT}, \ldots, \Delta P_{k1}$ to meet all the constraints with the latest load forecast:

$$P_{kt} = P^0_{kt} + \Delta P_{kt}(t = 1 \ldots T). \tag{8}$$

The corrected values will be determined to satisfy constraints (2)–(4) in the current time horizon (Fig. 1, step 14). These $P_{kt}(t = T \ldots 1)$ then will be treated as base GS in the next time horizon as explained before. It is noted that P^0_{kt} is based on the old load forecast $\hat{P}^0_t$, while P_{kt} on the latest forecast $\hat{P}_t$ implying that $\Delta P_{kT}, \ldots, \Delta P_{k1}$ absorbs the above-mentioned forecast errors by the supply-demand constraints as follows:

$$\sum_{k=1}^{N} \Delta P_{kt} = \hat{P}_t - \hat{P}^0_t \quad (t = 1 \ldots T) \tag{9}$$

where $\hat{P}_1 \equiv \hat{P}^0_1$.

C. Main Algorithm

In this section, we describe the details for the correction of base GS described in Section II-B4). A new ramp rate variable ΔD_{kt} is defined as follows:

$$\Delta D_{kt} = \Delta P_{kt} - \Delta P_{k(t+1)}. \tag{10}$$

In the proposed method, $\Delta D_{k1}, \Delta D_{k2} \ldots \Delta D_{kT}$ are determined in stages in backward direction from $t = 1 \ldots T$ using the equal λ method (Fig. 1, step 7). Fig. 3 shows the situation at the stage $t = s$, where $\Delta D_{k1}, \ldots, \Delta D_{k(s-1)}$ have already been computed giving an updated GS shown by dotted line. ΔD_{ks} is to be determined assuming that $\Delta D_{kt} = 0$ for $t > s$. In other words, the assumption of

$$\Delta P_{k(s+1)} \equiv 0 \tag{11}$$

is used in the determination of ΔD_{ks}. Note that a key issue of the proposed main algorithm is that only $\Delta D_{ks}(k = 1 \ldots N)$ are treated as variables. At this stage, the change in the value of ΔD_{ks} affects all $\Delta P_{kt}, t = 1 \ldots s$, governed by the following equation derived from the above definition:

$$\Delta P_{kt} = \sum_{j=t}^{s} \Delta D_{kj} = \Delta D_{ks} + \sum_{j=t}^{s-1} \Delta D_{kj} \quad (t = 1 \ldots s). \tag{12}$$

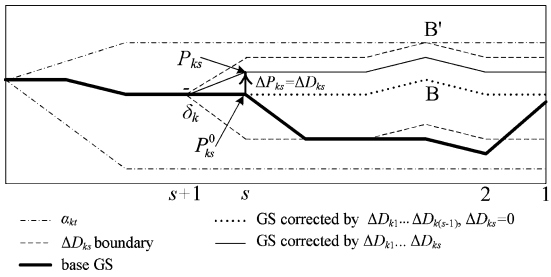

Fig. 3. Correction of base GS in the main algorithm.

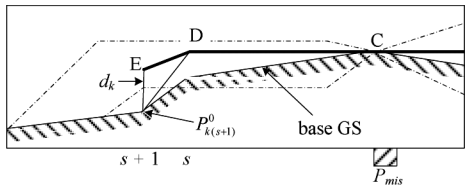

Fig. 4. Correction of $P^0_{k(s+1)}$ in the auxiliary algorithm.

When ΔD_{ks} is changed, the GS at $t = 1 \ldots s$ will either move up or down in parallel according to (12), limited by the boundary shown by dashed lines in Fig. 3.

The upper and lower bounds ($\overline{\Delta D}_{ks}$ and $\underline{\Delta D}_{ks}$) for ΔD_{ks} are set to satisfy both of the following constraints [refer to (32)].

- Constraint β : ramp-rate at s with respect to $(s+1)$.
- Constraint H : dispatch values of (12) at $t = 1 \ldots s$ must lie inside the FOR.

Fig. 3 shows an example, where upper limit $\overline{\Delta D}_{ks}$ is dictated at point B by upper limit B' (constraint H), and the lower limit $\underline{\Delta D}_{ks}$ is dictated by the ramp-rate limit (constraint β).

Supply-demand balance constraint for ΔD_{ks} is obtained from (9) and (10) as follows:

$$\sum_{k=1}^{N} \Delta D_{ks} = \varepsilon_s \tag{13}$$

where

$$\varepsilon_s = \left(\hat{P}_s - \hat{P}_{s+1}\right) - \left(\hat{P}^0_s - \hat{P}^0_{s+1}\right). \tag{14}$$

The above equation guarantees that the load and renewable energy forecast errors are absorbed at time point s and that, at the end of the algorithm, the dispatch results will satisfy supply-demand balance (2).

Under the above constraints, ΔD_{ks} will be calculated to minimize the overall total cost at $t = 1 \ldots s$. The optimization problem to determine ΔD_{ks} is one of main subjects in this paper. A solution method will be proposed using the equal λ method subroutine in Section III-C.

All the description above constitutes the main algorithm corresponding to step 5, 6, 7, 12, 13, and 14 in Fig. 1. As a summary, the algorithm starts from $s = 1$ (step 5), followed by the calculation of upper and lower limits (step 6) and then determination of ΔD_{ks} using the equal λ method (step 7). Then, we update s (step 12) and repeat the whole process until $s = T$ (step 13) and finally obtain the new GS (step 14).

D. Auxiliary Algorithm

Auxiliary algorithm is executed only when the main algorithm described in Section II-C cannot deal with the balance constraint (13). In this case, the equal λ method (Fig. 3, step 7) will produce non-zero mismatch value defined by

$$D_{mis} = \sum_{k=1}^{N} \Delta D_{ks} - \varepsilon_s. \tag{15}$$

Such non-zero mismatch tends to occur when FOR is reduced due to rapid change in loads or due to limited capability of existing generators. Fig. 4 shows a typical situation where at stage $t = s$, the main algorithm generates non-zero D_{mis} and GS corrected by ΔD_{ks} is given by a bold line CD. In this case, the bold line cannot move either up or down since it passes a single fixed point C in the FOR, resulting in non-zero D_{mis}.

In order to compensate non-zero D_{mis}, it is necessary to assume that $P^0_{k(s+1)}$ can be changed to absorb D_{mis}. Therefore, the equal λ method is performed in the auxiliary algorithm at point $(s+1)$ to determine the correction amount, d_k, needed for the original $P^0_{k(s+1)}$. This is shown by the bold line DE between s and $(s+1)$ in Fig. 4. The constraints necessary for the computation of d_k are given as follows:

The upper and lower constraint for d_k is given by

- Constraint β' : ramp-rate limit at $(s+1)$ with respect to s taking into account the contribution of previously determined ΔD_{ks}.
- Constraint H' : $P^0_{k(s+1)} + d_k$ must lie inside the FOR.

Supply-demand balance constraint is set to absorb D_{mis} in (15) according to the following equation:

$$\sum_{k=1}^{N} d_k = -D_{mis}. \tag{16}$$

The details of the computation of d_k, upper and lower constraint, and supply-demand balance constraint will be given in Section III-E. After the computation of d_k, the base dispatch values are updated (Fig. 1, step 11) as follows:

$$P^0_{k(s+1)} \leftarrow P^0_{k(s+1)} + d_k. \tag{17}$$

Since the above d_k absorbs the mismatch of (16), the demand at $s+1$ is also updated so as to meet the supply-demand balance constraint as follows:

$$\hat{P}^0_{s+1} \leftarrow \hat{P}^0_{s+1} - D_{mis}. \tag{18}$$

The above procedure is inserted in the main algorithm as shown in Fig. 1, steps 8 to 11. When the FOR explained in Section II-B2 is properly computed, the auxiliary algorithm in general will successfully absorb D_{mis} so that P_{mis} becomes always zero ($P_{mis} \equiv 0$) in the computation of the equal λ method in Fig. 1, step 10.

III. Solution of DELD Problem Using Equal λ Method

This section shows that the equal λ method is useful to solve the optimization problem in the static ELD (P_{kt}), main algorithm (ΔD_{ks}), as well as in the auxiliary algorithm (d_k) even though their formulations are different.

A. Condition of Optimality for DELD Problem

Firstly, the Lagrange multipliers λ_t, $\nu_{kt}^{(i)}$ and $\mu_{kt}^{(i)}$ are introduced corresponding to constraints (2)–(4) to obtain the following Lagrangian function for the DELD problem for time interval of $t = 1 \dots s$:

$$\begin{aligned} L(s) = \sum_{t=1}^{s} \Bigg\{ & f_t + \lambda_t \left(\hat{P}_t - \sum_{k=1}^{N} P_{kt} \right) \\ & + \sum_{k=1}^{N} \Big[\nu_{kt}^{(1)} \left(P_{kt} - \bar{P}_k \right) + \nu_{kt}^{(2)} \left(_k - P_{kt} \right) \\ & + \mu_{kt}^{(1)} \left(-\delta_k + P_{kt} - P_{k(t+1)} \right) \\ & + \mu_{kt}^{(2)} \left(-\delta_k - P_{kt} + P_{k(t+1)} \right) \Big] \Bigg\}. \end{aligned} \tag{19}$$

The above equation with $s = T$ implies the original problem defined in (1)–(4). Considering the Kuhn-Tucker necessary condition ($\partial L(s)/\partial P_{kt} = 0$) for (19), and introducing the following notations:

$$\nu_{kt} = \nu_{kt}^{(1)} - \nu_{kt}^{(2)}, \mu_{kt} = \mu_{kt}^{(1)} - \mu_{kt}^{(2)} \tag{20}$$

the necessary condition for optimality is written as follows:

$$a_k P_{kt} + b_k = \lambda_t U - \nu_{kt} - \mu_{kt} + \mu_{k(t-1)}. \tag{21}$$

If $k = 1 \dots N$ is expressed in vector form, (21) can be rewritten as follows:

$$AP_t + b = \lambda_t U - \nu_t - \mu_t + \mu_{t-1} (t = 1 \dots s) \tag{22}$$

where

$$\left. \begin{array}{c} U = [1 \cdots 1]^T, \nu_t = [\nu_{1t} \cdots \nu_{Nt}]^T \\ \mu_t = [\mu_{1t} \cdots \mu_{Nt}]^T \end{array} \right\}. \tag{23}$$

B. Equal λ Method

If we pay attention to only time point t, ramp-rate limits and their multipliers μ_t, μ_{t-1} can be eliminated as follows:

$$AP_t + b = \lambda_t U - \nu_t \quad (t = 1 \dots T). \tag{24}$$

If (24) is written in term of the elements of the vector, we have the following well-known expression of the equal λ criteria:

$$\lambda_t = a_1 P_{1t} + b_1 + \nu_{1t} = \cdots = a_N P_{Nt} + b_N + \nu_{Nt}. \tag{25}$$

This condition corresponds to a static ELD problem with objective function f_t in (1) subject to the supply-demand balance constraint (2) and the upper and lower constraint (3) for time point t. The conventional software for the problem, referred to as the equal λ method, will be fully utilized in the proposed method. The use of the equal λ method subroutine is expressed in this paper as in the following form, corresponding to (24):

$$(P_t, P_{mis}) = \lambda(\hat{P}_t, \bar{P}, \underline{P}, A, b). \tag{26}$$

In this expression, the input variables are given in the right-hand side, which are the demand in (2), vectors of upper and lower limits ($\bar{P}$, $\underline{P}$) in (3), and coefficients matrix in (1). The solution of (24) for the input variables are provided as output variables in the left-hand side, which are the result of load dispatch P_{kt} and the SDM defined by

$$P_{mis} = \sum_{k=1}^{N} P_{kt} - \hat{P}_t. \tag{27}$$

Note that variables λ_t and ν_t in (24) may be computed inside the equal λ method of (26), but they are not useful and eliminated from output variables. When the problem corresponding to (24) is infeasible, such as when the demand exceeds the total capacity of committed generators, a non-zero value for P_{mis} is provided together with P_{kt} within the limits.

C. Condition of Optimality for the Determination of ΔD_{ks}

This section derives the optimality condition for the determination of ΔD_{ks} under the assumption in the main algorithm.

If we add all the elements corresponding to $t = 1 \dots s$ in (22), we have the following equation:

$$A \left(\sum_{t=1}^{s} P_t \right) + sb = \left(\sum_{t=1}^{s} \lambda_t \right) U - \left(\sum_{t=1}^{s} \nu_t + \mu_s \right). \tag{28}$$

Now, $P_t = [P_{1t} \cdots P_{Nt}]^T$ in (28) is substituted by P_{kt} of (8) and then further substituted by ΔP_{kt}, $(k = 1 \dots N)$ of (12). This will replace the terms P_{kt} and ΔP_{kt}, in (28) with $\Delta D_t (t = 1 \dots s)$. Finally, dividing both sides of the equation with s, we have the following equation:

$$A \Delta D_s + (F_s + b) = \left(\frac{1}{s} \sum_{t=1}^{s} \lambda_t \right) U - \frac{1}{s} \left(\sum_{t=1}^{s} \nu_t + \mu_s \right) \tag{29}$$

where

$$\left. \begin{array}{c} F_s = \frac{A}{s} \left(\sum_{m=1}^{s-1} \sum_{t=m}^{s-1} \Delta D_t + \sum_{t=1}^{s} P_t^0 \right) \\ = \frac{1}{s} \left((s-1) F_{s-1} + A \left((s-1) \Delta D_{s-1} + P_s^0 \right) \right), \\ F_1 = A P_1^0 \end{array} \right\}. \tag{30}$$

As explained in Section II-C, the assumption in the main algorithm is that $\Delta D_s = [\Delta D_{1s} \cdots \Delta D_{Ns}]^T$ is the only decision variable vector; while the other terms $\Delta D_1, \dots, \Delta D_{s-1}$ constituting F_s are treated as fixed values in the sequential optimization process (Fig. 1, steps 5 and 12). Instead of computing ΔP_t simultaneously for $t = 1 \dots T$, we calculate sequentially ΔD_s at every $t = s (s = 1 \dots T)$. The resulting ΔP_t, at $t = 1 \dots s$, will depend on the correction ΔD_s at $t = s$ based on (12). The sequential determination of $\Delta D_1, \dots, \Delta D_s$ will automatically satisfy all the ramp-rate constraints. An important observation is that condition (29) is exactly the same form as condition (24) of the equal λ method, implying that the solution can be efficiently obtained by a very fast algorithm [14] for the conventional equal λ method as in the following manner:

$$(\Delta D_s, D_{mis}) = \lambda \left(\varepsilon_s, \overline{\Delta D}_s, \underline{\Delta D}_s, A, (F_s + b) \right). \tag{31}$$

ΔD_{ks} will be determined such that the total cost at $t = 1 \dots s$ is minimized. Input variable ε_s is previously defined in (14) corresponding to the balance constraint for ΔD_k. Variables ($\overline{\Delta D}$, $\underline{\Delta D}$), the vectors of upper and lower limits, will be

detailed in the next section. A and $(F_s + b)$ are the coefficients for the s optimality condition of (28). The equal λ method (31) solves the optimality condition under the above specified inputs to provide the output variables in the left-hand side of (31). Note that the proposed method is suboptimal due to the assumption of the main algorithm. In other words, the method is optimal under the assumption of the main algorithm.

D. Upper and Lower Limits for the Main Algorithm

The upper and lower limits in (31) are determined by constraint β and H where we denote the upper and lower limits as $(\bar{\beta}_{ks}, \underline{\beta}_{ks})$ and $(\bar{H}_{ks}, \underline{H}_{ks})$, respectively. We use the following setting in the real-time algorithm (Fig. 1, step 6):

$$\left.\begin{aligned}\overline{\Delta D}_{ks} &= \min\left[\bar{\beta}_{ks}, \max\left(\bar{H}_{ks}\underline{\beta}_{,ks}\right)\right] \\ \underline{\Delta D}_{ks} &= \max\left[\underline{\beta}_{ks}, \min\left(\underline{H}_{ks}, \bar{\beta}_{ks}\right)\right]\end{aligned}\right\}. \tag{32}$$

The above limits $(\overline{\Delta D}_{ks}, \underline{\Delta D}_{ks})$ define the range that satisfy both constraint β and H mentioned before in Section II-C. Due to the assumption (11), there will be sometimes a case when the range that satisfies both constraints simultaneously does not exist. For example, when $\underline{\beta} > \bar{H}_{ks}$ and the range does not exist, the setting of (32) provides $\overline{\Delta D}_{ks} = \underline{\Delta D}_{ks} = \underline{\beta}_{ks}$ to guarantee the solution, where we adopt a strategy that non-zero D_{mis} is intentionally generated as mentioned in Section II-D. Setting for $(\bar{\beta}_{ks}, \underline{\beta}_{ks})$ and $(\bar{H}_{ks}, \underline{H}_{ks})$ in (32) are given as below.

Constraint β is a ramp-rate constraint between $t = s$ and $t = s + 1$ as follows (Fig. 1, step 6):

$$\left.\begin{aligned}\bar{\beta}_{ks} &= \delta_k - P^0_{ks} + P^0_{k(s+1)} \\ \underline{\beta}_{ks} &= -\delta_k - P^0_{ks} + P^0_{k(s+1)}\end{aligned}\right\}. \tag{33}$$

Constraint H implies the margin to the bound such that dispatch values at $t = 1 \ldots s$ lie inside the FOR as explained before in Fig. 3. For example, distance BB', the shortest distance point among $t = 1 \ldots s$, governs the upper limit of constraint H. Since the main algorithm identifies such a critical constraint successively, we adopt the following form that compares the critical value in the previous stage $s - 1$ and the margin at the studied point s (Fig. 1, step 12):

$$\left.\begin{aligned}\bar{H}_{ks} &= \min\left[\left(\bar{H}_{k(s-1)} - \Delta D_{k(s-1)}\right), \left(\bar{\alpha}_{ks} - P^0_{ks}\right)\right] \\ \underline{H}_{ks} &= \max\left[\left(\underline{H}_{k(s-1)} - \Delta D_{k(s-1)}\right), \left(\underline{\alpha}_{ks} - P^0_{ks}\right)\right]\end{aligned}\right\} \tag{34}$$

where $\bar{H}_{k1} = \bar{\alpha}_{k1} - P^0_{k1}$, $\underline{H}_{k1} = \underline{\alpha}_{k1} - P^0_{ks}$ is the initial value at $s = 1$ (Fig. 1, step 5).

E. Detail of the Auxiliary Algorithm

The auxiliary algorithm is outlined in Section II-D. The algorithm modifies the base dispatch value $P^0_{k(s+1)}$ by the amount d_k at $t = (s + 1)$ as expressed in (17). Therefore, the optimality condition for correction d_k may be obtained by substituting $(P^0_{s+1} + d)$ into P_t in (24) as follows:

$$A\left(P^0_{s+1} + d\right) + b = Ad + \left(AP^0_{s+1} + b\right) = \lambda_{s+1}U - \nu_{s+1}. \tag{35}$$

TABLE I
GENERATORS DATA

Unit's number, k	$\overline{P}_k$ (MW)	$\underline{P}_k$ (MW)	δ_k (MW/min)	a_k ¥/MW^{2}h	b_k ¥/MWh	c_k ¥/h
1	1900	600	1	0.00035	0.4	1100
2	600	105	1	0.00016	1.3	182
3	1300	280	3	0.00020	2.4	234
4	300	160	3	0.00125	2.2	132
5	2700	700	5	0.000095	5.0	1040
6	900	200	5	0.000025	5.0	400
Total	7700	2045	18			

From the above optimality condition, it follows that correction $d = [d_1 \ldots d_N]^T$ is obtained by the equal λ method subroutine as in the following manner (Fig. 1, step 10):

$$(d, P_{mis} \equiv 0) = \lambda\left(-D_{mis}, \bar{d}, \underline{d}, A, \left(AP^0_{s+1} + b\right)\right) \tag{36}$$

where $\bar{d} = \left[\bar{d}_1 \cdots \bar{d}_N\right]$ and $\underline{d} = \left[\underline{d}_1 \cdots \underline{d}_N\right]$. In the above computation, non-zero input of mismatch $(-D_{mis})$ will be absorbed to guarantee the balance constraint $(P_{mis} = 0)$ in condition that the FOR have been accurately computed as explained before.

The upper and lower limits (Fig. 1, step 9), $\bar{d}_k$ and $\underline{d}_k$ are set as the overlapping area of β and H' as mentioned in Section II-D as follows:

$$\left.\begin{aligned}\bar{d}_k &= \min\left[\left(\Delta D_{ks} - \underline{\beta}_{ks}\right), \left(\bar{\alpha}_{k(s+1)} - P^0_{k(s+1)}\right)\right] \\ \underline{d}_k &= \max\left[\left(\Delta D_{ks} - \bar{\beta}_{ks}\right), \left(\underline{\alpha}_{k(s+1)} - P^0_{k(s+1)}\right)\right]\end{aligned}\right\}. \tag{37}$$

F. Summary of the Proposed Algorithm

As shown in Fig. 1, the main algorithm is very simple and the computation time is steady and consistent. Furthermore, the algorithm is robust and useful even after system breakdown. Any base dispatch values are useful as an initial GS to be updated if it is inside the FOR.

IV. CASE STUDIES

A. Simulation Data

As is mentioned in the Introduction, the proposed method is developed for a system with restricted load following capability suffering from rapid change in loads. In order to verify the effectiveness of the proposed method, we use six thermal power plants, with each combined capacities shown in Table I.

Four demand patterns representing two hours load curve around morning to noon are shown in Fig. 5. The renewable energy is treated as negative load in the proposed algorithm. The disturbance caused by the renewable energy is characterized by the presence of rapid change in load. There will be some case where the rapid increase or decrease in load cannot be matched by the generators' capability resulting in no FOR. This is detected by the presence of SDM. Therefore, we use Demand Pattern 4 to represent the case where SDM will occur.

The time horizon is assumed to be one hour ahead $(T = 12)$ and the forecasted demand, $\hat{P}_{12} \ldots \hat{P}_1$, is avail-

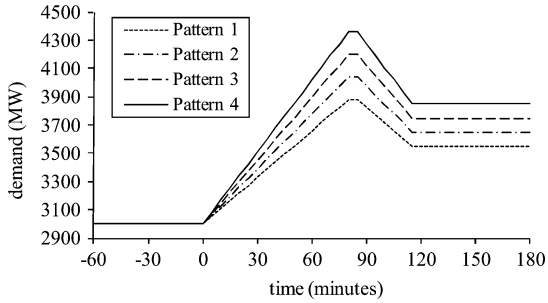

Fig. 5. Two hours demand pattern with preceding and succeeding one-hour constant demand.

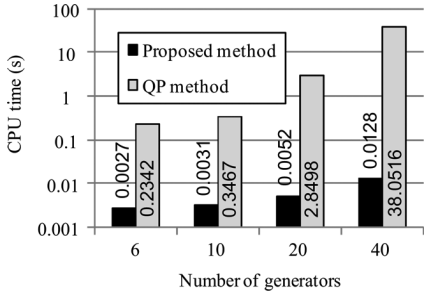

Fig. 6. Comparison of CPU time.

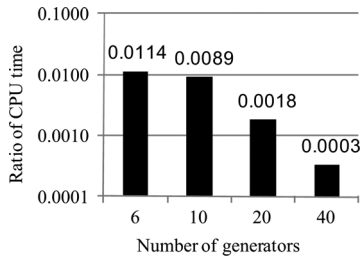

Fig. 7. Ratio of proposed method's CPU time to QP methods CPU time.

able in 5-min interval in the time horizon, where load forecast errors are neglected. Constant artificial demand $\hat{P}_t = 3000$ MW $(t = 12 \ldots 1)$ and its optimal dispatch values are used as GS in the initial time horizon $(-60 \ldots 0$ min) for the sake of smooth start, corresponding to Fig. 1, step 0.

Furthermore, to verify the robustness of the proposed method and for the purpose of CPU time comparison, the proposed method is also tested on 3-generator system [15], 10-generator system [12], and 40-generator system [16]. The 20-generator system was also used by doubling the 10-generator system. The demand pattern was scaled up depending on the system capacity. The 40-generator system was also tested with demand consisting renewable energy generation.

The proposed method will be compared with the quadratic programming (QP) method under the same real-time operation condition. The QP method optimizes the generation cost of all intervals in the entire time horizon simultaneously using MATLAB's quadprog algorithm. In case when the demand is infeasible, there will be no feasible results with normal QP method. To overcome this, a slack generator with high cost is added to the system. The slack generator will only generate positive or negative output when the demand is infeasible indicating the amount of SDM.

B. Results and Discussion

The characteristic of each compared method is remarkably obvious for the dispatch of demand pattern 4 in the 6-generator system, which has the most severe change in demand. Particular simulation results for generator 2, which is the most ramp-rate restricted generator, are tabulated in Table II in terms of the changes of GS and SDM. The comparison of SDM between the proposed method and QP with slack generator method for 3-generator system is shown in Table III. The summary of the overall results for 6-generator system is shown in Table IV. In Figs. 6 and 7, the comparison on the CPU time for 6-, 10-, 20-, and 40-generator system are presented. In the following subsections, the explanations and discussions for the results are presented.

1) Transition of Expected Dispatch Value: Table II(a) column (1) lists GS calculated at $time = -20$ min for the 6-generator system. The underlined value (222 MW) is the current active power output of generator 2 at $time = -20$ min, and the remaining values are expected GS within one hour ahead. As the time progress by 5 min, GS at $time = -15$ min will become the active power output of generator 2 in the new time horizon beginning at $time = -15$ min [Table II(a) column (2)].

For the proposed method, if we compare column (1) and (2), with respect to time, the dispatch values are the same. For example, at $time = -15$ min, GS is 212 MW in both column (1) and (2), implying no change in GS. In general, the change in GS is necessary to cope with unpredictable load change but it will give additional burden to operators as well as to the system. If the change is necessary, it is preferable from the viewpoint of power system operation that the amount is larger for the further future and smaller for the near future.

If we observe the GS in Table II(a), the change (bold numeric) is only seen at the furthest future of the time horizon. This is due to the algorithm of the proposed method, where the correction starts from the furthest future $(t = 1)$ and therefore, coming towards the near future $(t = T)$, the amount of change becomes smaller. In this way, the proposed method is convenient to the system operator and preferable for the system. This is the characteristic 3) mentioned in Section I.

2) Guaranteed Supply-Demand Balance, Transition of Expected Supply-Demand Mismatch: The numerical value inside (.) in Table II is the expected SDM. In both of the proposed method and quadratic programming method, the numerical value inside (.) is zero and supply-demand balance up to one hour ahead is maintained. However, the FOR does not exist due to the severe change in demand pattern 4, which exceeds the generators' capability. This is seen in column (5) onwards for the proposed method in Table II(a) and column (4) for the QP in Table II(b). The difference between the methods comes from the different pattern of GS transitions. In this case, the proposed method detect the 10 MW SDM at the furthest point $time = 75$ min in the time horizon beginning at $time = 15$ min as mentioned by the formulation in Section II-B2. If the SDM is compensated by the reserve in the system, the FOR can be secured and GS can be computed. In the normal QP method,

TABLE II
GS TRANSITION OF GEN 2 AND SDM FOR DEMAND PATTERN 4 (6-GENERATOR SYSTEM). (A) PROPOSED METHOD. (B) NORMAL QP METHOD. (C) QP METHOD WITH SLACK GENERATOR

time	(1)	(2)	(3)	(4)	(5)	(6)	(7)
-20	222 (0)						
-15	217 (0)	217 (0)					
-10	212 (0)	212 (0)					
-5	207 (0)	207 (0)	207 (0)				
0	202 (0)	202 (0)	202 (0)				
5	207 (0)	207 (0)	207 (0)				
10	212 (0)	212 (0)	212 (0)	212 (0)			
15	217 (0)	217 (0)	217 (0)	217 (0)	217 (0)		
20	222 (0)	222 (0)	222 (0)	222 (0)	222 (0)		
25	227 (0)	227 (0)	227 (0)	227 (0)	227 (0)		
30	232 (0)	232 (0)	**227** (0)	**232** (0)	232 (0)		
35	237 (0)	237 (0)	**227** (0)	**237** (0)	237 (0)		
40	242 (0)	242 (0)	**227** (0)	**242** (0)	242 (0)		
45		247 (0)	**227** (0)	**247** (0)	247 (0)		
50			**227** (0)	**252** (0)	252 (0)		
55			227 (0)	**257** (0)	257 (0)	257 (0)	
60				**262** (0)	262 (0)	262 (0)	
65				**267** (0)	267 (0)	267 (0)	
70				272 (0)	272 (0)	272 (0)	
75					277 (10)	277 (10)	277 (10)

(a)

time	(1)	(2)	(3)	(4)	(5)	(6)	(7)
-20	257 (0)						
-15	257 (0)	257 (0)					
-10	257 (0)	257 (0)					
-5	259 (0)	**260** (0)	261 (0)				
0	264 (0)	**265** (0)	**266** (0)				
5	269 (0)	**270** (0)	**271** (0)				
10	274 (0)	**275** (0)	**276** (0)	No			
15	279 (0)	**280** (0)	**281** (0)	solution			
20	284 (0)	**285** (0)	**286** (0)				
25	289 (0)	**290** (0)	**291** (0)				
30	294 (0)	**295** (0)	**296** (0)				
35	299 (0)	**300** (0)	**301** (0)				
40	304 (0)	**305** (0)	**306** (0)				
45		310 (0)	**311** (0)				
50			316 (0)				
55			321 (0)				
60							
65							
70							
75							

(b)

time	(1)	(2)	(3)	(4)	(5)	(6)	(7)
-20	257 (0)						
-15	257 (0)	257 (0)					
-10	257 (0)	257 (0)					
-5	259 (0)	**260** (0)	261 (0)				
0	264 (0)	**265** (0)	**266** (0)				
5	269 (0)	**270** (0)	**271** (0)				
10	274 (0)	**275** (0)	**276** (0)	276 (0)			
15	279 (0)	**280** (0)	**281** (0)	281 (0)	281 (0)		
20	284 (0)	**285** (0)	**286** (0)	286 (0)	286 (0)		
25	289 (0)	**290** (0)	**291** (0)	291 (0)	291 (0)		
30	294 (0)	**295** (0)	**296** (0)	296 (0)	296 (0)		
35	299 (0)	**300** (0)	**301** (0)	301 (0)	301 (0)		
40	304 (0)	**305** (0)	**306** (0)	306 (0)	306 (0)		
45		310 (0)	**311** (0)	311 (0)	311 (0)		
50			316 (0)	316 (0)	316 (0)		
55			321 (0)	321 (0)	321 (0)	321 (0)	
60				326 (0)	326 (0)	326 (0)	
65				331 (0)	331 (0)	331 (0)	
70				336 (10)	336 (10)	336 (10)	
75					341 (20)	341 (20)	341 (20)

(c)

there will be no feasible solution in column (4) due to infeasible demand [Table II(b)]. For the QP method with slack generator, 10 MW SDM is detected in column (4) of Table II(c), shown by the numerical value inside (.).

If we observe the transition of the 10 MW expected SDM generated at $time = 75$ min, we can see that the values do not change at all in column (5) to column (7) of Table II(a) (shaded numeric). The actual SDM of 10 MW will be encountered at

TABLE III
GS TRANSITION OF GEN 2 AND SDM FOR DEMAND PATTERN 4[15]

	Proposed method			QP method with slack generator		
time	(1)	(2)	(3)	(4)	(5)	(7)
45	85 (0)			85 (0)		
50	70 (-10)	70 (-10)		70 (-10)	70 (-10)	
55	55 (-5)	55 (-5)	55 (-5)	55 (-5)	55 (-5)	55 (-5)
60	50 (0)	50 (0)	50 (0)	50 (0)	50 (0)	50 (0)
65	50 (0)	60 (0)	60 (0)	50 (0)	62.5 (-2.5)	62.5 (-2.5)
70	65(0)	75 (0)	75 (0)	65 (0)	77.5 (0)	77.5 (0)
75	80 (0)	90 (0)	90 (0)	80 (0)	92.5 (0)	92.5 (0)
80	95 (0)	105 (0)	105 (0)	95 (0)	107.5 (0)	107.5 (0)
85	110 (0)	120 (0)	120 (0)	110 (0)	122.5 (0)	122.5 (0)
90	125 (0)	135 (0)	135 (0)	125 (0)	137.5 (0)	137.5 (0)
95	140 (0)	150 (0)	150 (0)	140 (0)	152.5 (0)	152.5 (0)
100	155 (0)	165 (0)	165 (0)	155 (0)	167.5 (0)	167.5 (0)
105	170 (0)	180 (0)	180 (0)	170 (0)	182.5 (0)	182.5 (0)
110		195 (5)	195 (5)		197.5 (2.5)	197.5 (2.5)
115			210 (0)			212.5 (0)

TABLE IV
PERFORMANCE COMPARISON OF THE 6-GENERATOR SYSTEM

Demand pattern	Proposed method			QP method with slack generator		
	Fuel cost (¥) (a)	SDM (MW) (b)	CPU time (s) (c)	Fuel cost (¥) (a)	SDM (MW) (b)	CPU time (s) (c)
1	119459	0.0	0.0029	118904	0.0	0.1923
2	124063	0.0	0.0026	123850	0.0	0.2963
3	128992	0.0	0.0025	128963	0.0	0.2140
4	134454	30.0	0.0027	134233	60.0	0.2832

$time = 75$ min as in column (7). In this example, both methods detected the SDM at the end of the time horizon. However, this is not guaranteed by the QP method as shown in the next section.

Table III shows the GS for generator 2 for 3-generator system and demand pattern 4 used in [15]. Shown in column (1) and (4) are the GS for the time horizon beginning at $time = 45$ min for proposed and QP method with slack generator, respectively. There are -10 and -5 MW SDM at $time = 50$ and 55 min, detected in previous time horizon shown inside (.). In the time horizon beginning at $time = 50$ min [column (2)], the proposed method detected 5 MW SDM at the end of the time horizon [underlined value in column (2)]. QP method on the other hand detected two SDM which is -2.5 MW at $time = 65$ min and 2.5 MW at $time = 110$ min [underlined value in column (5)]. The QP method detected SDM inside the time horizon, close to the current operating time. The proposed method is more desirable since the SDM is detected at the end of the time horizon, which will give more time to the operator to take necessary actions.

3) Generation Cost: Table IV column (a) shows the total fuel cost of the entire two hours for each demand pattern in the 6-generator system. Table IV column (b) lists the amount of total SDM generated in the actual operation. For demand pattern 4, the total SDM for the proposed method is 30 MW and the total SDM of QP method with slack generator is 60 MW. The numeric is the sum of actual SDM for the two hours demand pattern. The difference in SDM values between the methods comes from the different pattern of GS transitions.

The reason why the optimal QP method produces larger SDM is explained as follows. The optimization in each control cycle is constrained by the current operating point, which is a fixed starting point. However, the QP method and the proposed method provide different GS and therefore different operating points. Then, we will have two different optimization problems with different starting point constraints, where SDM totally depends on the starting point. As a result, the QP method may

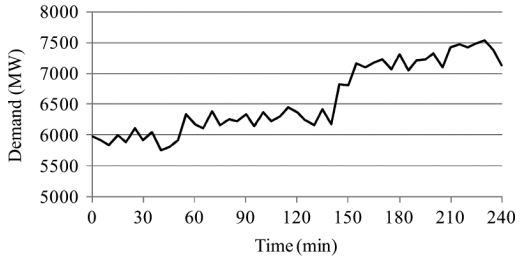

Fig. 8. Forecasted demand with renewable generation.

result in larger SDM for repeated use of starting point-constrained optimizations. Note that from Table II column (4), the starting point of generator 2 is 212 MW for the proposed method and 276 MW for the QP method. As a result, different SDM are detected. This explains the results in Table IV. Another point to be noted is that the QP method tries to minimize the total SDM in the specified time horizon, while the FOR algorithm in this paper in [13] tries to compute minimum SDM sequentially from the current operating point towards the future in order to maintain the FOR as large as possible. Due to this characteristic, the proposed method tends to provide less SDM compared with the QP method.

When we compare the costs between the methods for the cases where the SDM are zero, the proposed method is economically comparable with QP method.

4) CPU Time: The CPU time is presented in Table IV column (c) for every demand pattern in the 6-generator system. The CPU time represents the average computation time to determine the GS for a single time horizon. In the proposed method, the CPU time is constant about 0.0027 s, while in the QP method, the CPU time varies around 0.2 s influenced by the demand pattern. The computation was performed on Intel Core 2 Duo processor 3 GHz with 2 GB of RAM.

Fig. 6 shows the CPU time for 6-, 10-, 20-, and 40-generator systems. It is observed that the CPU time increases almost linearly with respect to the number of generators for the proposed method, while for the QP method, the increase is exponential. The ratio of CPU time for the proposed method to the QP method is shown in Fig. 7. As indicated in Fig. 7, the proposed method uses far less CPU time as compared to the QP method. It can be concluded that the proposed method is very fast and useful for real-time system with a large number of generators as compared to the QP method.

5) Case Study for Load With Renewable Energy Source: The proposed method was tested on 40-generator system against actual forecasted load and renewable energy generation (Fig. 8). The forecasted renewable energy generation is treated as negative load. The installed renewable generation capacity is 800 MW. The cost given by the proposed method is 323 760, and for the QP method, the cost is 323 280. The CPU time is 0.013 s for the proposed method and 34 s for the QP method.

V. Conclusion

With large penetration of renewable energy in future power system operations, increased uncertainty cannot be avoided even if various smart grid proposals are fully and successfully performed. In this situation, prediction errors will become larger and sudden change in operation conditions must be taken into account. In this case, the computation speed is a critical issue since frequent change in operation schedule in real-time operation will be inevitable to cope with the situation. The paper proposes a high-speed dynamic ELD method by utilizing the short-term load forecast. A new formulation fully utilizing the conventional equal λ method ensures fast and steady computation time. The method is suitable for power system with large renewable energy penetration suffering from large disturbances whose fluctuations might cause infeasibility and their prediction error requires continuous change in operation schedule. Supply-demand balance is maintained even for infeasible cases where minimum compensations are suggested to operators in advance to realize reliable power system operations.

Since the method is developed for vertical integrated system, the issues of its applications in the energy market environment have not been studied. There are possibly several future applications in such area since the method is to fully realize the supply and demand constraint in uncertain circumstances. The problem will be studied in the future.

References

[1] D. W. Ross and S. Kim, "Dynamic economic dispatch of generation," *IEEE Trans. Power App. Syst.*, vol. PAS-99, no. 6, pp. 2060–2068, Nov. 1980.

[2] T. Li and M. Shahidehpour, "Dynamic ramping in unit commitment," *IEEE Trans. Power Syst.*, vol. 22, no. 3, pp. 1379–1381, Aug. 2007.

[3] W. G. Wood, "Spinning reserve constrained static and dynamic economic dispatch," *IEEE Trans. Power App. Syst.*, vol. PAS-101, no. 2, pp. 381–388, Feb. 1982.

[4] D. N. Simopoulos, S. D. Kavatza, and C. D. Vournas, "Unit commitment by an enhanced simulated annealing algorithm," *IEEE Trans. Power Syst.*, vol. 21, no. 1, pp. 68–76, Feb. 2006.

[5] C. L. Chen, "Simulated annealing-based optimal wind-thermal coordination scheduling," *IET Gen., Transm., Distrib.*, vol. 1, no. 3, pp. 447–455, 2007.

[6] A. Y. Abdelaziz, M. Z. Kamh, S. F. Mekhamer, and M. A. L. Badr, "A hybrid HNN-QP approach for dynamic economic dispatch problem," *Elect. Power Syst. Res.*, vol. 78, no. 10, pp. 1784–1788, Oct. 2008.

[7] F. N. Lee, L. Lemonidis, and K. C. Liu, "Price-based ramp-rate model for dynamic dispatch and unit commitment," *IEEE Trans. Power Syst.*, vol. 9, no. 3, pp. 1233–1242, Aug. 1994.

[8] J. P. Chiou, "A variable scaling hybrid differential evolution for solving large-scale power dispatch problem," *IET Gen., Transm., Distrib.*, vol. 3, no. 2, pp. 154–163, 2009.

[9] C. B. Somuah and N. Khunaizi, "Application of linear programming redispatch technique to dynamic generation allocation," *IEEE Trans. Power Syst.*, vol. 5, no. 1, pp. 20–26, Feb. 1990.

[10] W. R. Barcelo and P. Rastgoufard, "Dynamic economic dispatch using the extended security constrained economic dispatch algorithm," *IEEE Trans. Power Syst.*, vol. 12, no. 2, pp. 961–967, May 1997.

[11] G. Irisarri, L. M. Kimball, K. A. Clements, A. Bagchi, and P. W. Davis, "Economic dispatch with network and ramping constrained via interior point methods," *IEEE Trans. Power Syst.*, vol. 13, no. 1, pp. 236–242, Feb. 1998.

[12] X. S. Han, H. B. Gooi, and D. S. Kirschen, "Dynamic economic dispatch: Feasible and optimal solutions," *IEEE Trans. Power Syst.*, vol. 16, no. 1, pp. 22–28, Feb. 2001.

[13] H. M. Hafiz, N. Yorino, Y. Sasaki, and Y. Zoka, "Feasible operation region for dynamic economic load dispatch and reserve monitoring," *Eur. Trans. Elect. Power*, to be published.

[14] R. R. Shoults, S. K. Chang, S. Helmick, and W. M. Grady, "A practical approach to unit commitment, economic dispatch and saving allocation for multi-area pool operation with import/export constraints," *IEEE Trans. Power App. Syst.*, vol. PAS-99, no. 2, pp. 625–635, Mar./Apr. 1980.

[15] N. Yorino, H. M. Hafiz, Y. Zoka, Y. Sasaki, A. Sudo, and Y. Ohnishi, "Dynamic economic dispatch with generator's feasible operation region," in *Proc. Asia-Pacific Power and Energy Engineering Conf. (APPEEC) 2010*, Chengdu, China, 2010.

[16] N. Sinha, R. Chakrabarti, and P. K. Chattopadhyay, "Evolutionary programming techniques for economic load dispatch," *IEEE Trans. Evol. Computat.*, vol. 7, no. 1, pp. 83–94, Feb. 2003.

Naoto Yorino (M'90) received the B.S., M.S., and Ph.D. degrees in electrical engineering from Waseda University, Shinjuku, Japan, in 1981, 1983, and 1987, respectively.

He is a Professor in the Graduate School of Engineering, Hiroshima University, Hiroshima, Japan. He was with Fuji Electric Co. Ltd., Japan, from 1983 to 1984. He was a Visiting Professor at McGill University, Montreal, QC, Canada, from 1991 to 1992.

Dr. Yorino is a member of the IEE of Japan, CIGRE, iREP, and ESCJ.

Habibuddin M. Hafiz (S'01) received the B.Eng. and M.Eng. degrees in electrical engineering from Universiti Teknologi Malaysia, Johor, Malaysia, in 2001 and 2003, respectively.

He has been a Lecturer in the Faculty of Electrical Engineering, Universiti Teknologi Malaysia, Johor, Malaysia, since 2003 and is now on study leave.

Yutaka Sasaki (M'08) received the Ph.D. degree in information science from Hokkaido University, Sapporo, Japan, in 2008.

Since 2008, he has been an Assistant Professor at Hiroshima University, Hiroshima, Japan. His research interests include optimal planning and operation of distributed generations.

Yoshifumi Zoka (M'99) received the B.S., M.S., and Ph.D. degrees from Hiroshima University, Hiroshima, Japan, in 1995, 1997, and 2002, respectively.

He was a Visiting Scholar at the University of Washington, Seattle, from 2002 to 2003. He is currently an Associate Professor at the Graduate School of Engineering, Hiroshima University. His research interests are power system planning, stability, and control problems.

Dr. Zoka is a member of the IEE of Japan.